





Cite this: *RSC Adv.*, 2017, 7, 31767

# Incorporating a TiO<sub>x</sub> shell in single-walled carbon nanotube/fullerodendron coaxial nanowires: increasing the photocatalytic evolution of H<sub>2</sub> from water under irradiation with visible light†

K. Kurniawan,<sup>a</sup> T. Tajima,<sup>a</sup> <sup>\*,a</sup> Y. Kubo,<sup>a</sup> H. Miyake,<sup>b</sup> <sup>b</sup> W. Kurashige,<sup>c</sup> Y. Negishi <sup>c</sup> and Y. Takaguchi <sup>\*,a</sup>Received 13th May 2017  
Accepted 13th June 2017

DOI: 10.1039/c7ra05412b

rsc.li/rsc-advances

A custom-tailored single-walled carbon nanotube (SWCNT) photocatalyst with an electron-extracting TiO<sub>x</sub> shell, i.e., a SWCNT/fullerodendron/TiO<sub>x</sub> coaxial nanowire, has been fabricated. Due to the presence of the TiO<sub>x</sub> shell, the SWCNT/fullerodendron/TiO<sub>x</sub> coaxial nanowire shows an enhanced photocatalytic activity ( $\Phi = 0.47$ ) for the evolution of hydrogen from water under irradiation with visible light ( $\lambda = 450$  nm).

The interfaces between metal oxides and organic compounds play an important role in the field of organic electronics, which include organic light-emitting devices (OLEDs),<sup>1,2</sup> organic photovoltaic cells (OPVs),<sup>1,3</sup> dye-sensitized solar cells (DSSCs),<sup>1c</sup> and transistors.<sup>4</sup> To improve the device performance, these interfaces can often be modified by insertion of a functional interfacial layer. For example, transparent titanium oxides (TiO<sub>x</sub>) exhibit electronic levels that match the LUMOs of the C<sub>60</sub>-derivatives used in OPVs well, which renders TiO<sub>x</sub> a promising candidate for electron-transport materials.<sup>5,6</sup> Waldauf and co-workers have prepared OPVs with an ITO/TiO<sub>x</sub>/RR-P3HT:PCBM/PEDOT:PSS/Au structure using coating techniques, and demonstrated that these OPVs exhibit improved fill factors (FF).<sup>5</sup> Kuwabara *et al.* have reported efficient inverted BHJ solar cells that contain TiO<sub>x</sub> as the electron-extraction layer,<sup>6</sup> which resulted in an improved short-circuit photocurrent ( $J_{sc}$ ), open-circuit voltage ( $V_{oc}$ ), FF, and power-conversion efficiency ( $\eta$ ).

Meanwhile, coaxial nanowires with a donor-acceptor heterojunction have shown great potential for applications in innovative photofunctional materials. Recent theoretical<sup>7</sup> and experimental<sup>8</sup> studies have indicated that coaxial nanowire structures could potentially improve the carrier collection and overall efficiency relative to bulk semiconductors of the same materials. We have reported the fabrication and efficient photo-

induced electron-transfer processes of single-walled carbon nanotube (SWCNT)/anthryl dendron<sup>9,10</sup> and SWCNT/fullerodendron supramolecular nanocomposites,<sup>9,11</sup> wherein a coaxial nanowire structure provides a donor-acceptor heterojunction between the SWCNT-core and the C<sub>60</sub>-based fullerodendrons. We have also shown that SWCNT/fullerodendron ( $\Phi = 0.28$ ) and SWCNT/fullerodendron/SiO<sub>2</sub> ( $\Phi = 0.31$ ) coaxial nanohybrid materials can be used as effective photosensitizers for the catalytic evolution of H<sub>2</sub> from water under irradiation with visible light ( $\lambda = 450$  nm).<sup>12</sup> Moreover, we have reported the direct incorporation of a co-catalyst into the shell of SWCNT/fullerodendron supramolecular nano-composites.<sup>13</sup> Upon chirality-selective photo-excitation using monochromatic light ( $\lambda = 680$  nm), which is suitable for the  $E_{22}$  absorption of (8,3) SWCNTs, we observed the first example for the evolution of H<sub>2</sub> ( $\Phi = 0.015$ ) photosensitized by SWCNTs.<sup>14</sup> However, further improvements of the quantum yield of the SWCNT photocatalyst are necessary in order to further develop this technology.

These results prompt us to explore a new coaxial photosensitizer with a TiO<sub>x</sub> shell as an electron-extraction layer that covers a photo-functional SWCNTs/C<sub>60</sub> interface. Here we describe the fabrication of SWCNT/fullerodendron/TiO<sub>x</sub> coaxial nano-hybrids that can be used for the effective photo-catalytic evolution of H<sub>2</sub>, which shows the highest AQYs ( $\Phi = 0.47$ ) under irradiation with visible light ( $\lambda = 450$  nm).

The molecular structure of the fullerodendron used in the present study is shown in Fig. 1. SWCNT/fullerodendron/TiO<sub>x</sub> nano-hybrids were fabricated by a polycondensation reaction of titanium tetra isopropoxide (TTIP)<sup>15</sup> using SWCNT/fullerodendron supramolecular nano-composites (Fig. 1) as catalytic scaffolds according to previous reports on SWCNT/fullerodendron/SiO<sub>2</sub> nano-hybrids.<sup>12</sup> In a typical run, an aqueous solution of SWCNT/fullerodendron nanocomposites

<sup>a</sup>Graduate School of Environmental and Life Science, Okayama University, 3-1-1 Tsushima-Naka, Kita-ku, Okayama, 700-8530, Japan. E-mail: tajimat@cc.okayama-u.ac.jp; yutaka@cc.okayama-u.ac.jp

<sup>b</sup>Graduate School of Sciences and Technology for Innovation, Yamaguchi University, 2-16-1 Tokiwadai, Ube, Yamaguchi 755-8611, Japan

<sup>c</sup>Department of Applied Chemistry, Faculty of Science Division I, Tokyo University of Science, 1-3 Kagurazaka, Shinjuku-ku, Tokyo 162-8601, Japan

† Electronic supplementary information (ESI) available: Experimental procedure, Fig. S1–S7. See DOI: 10.1039/c7ra05412b

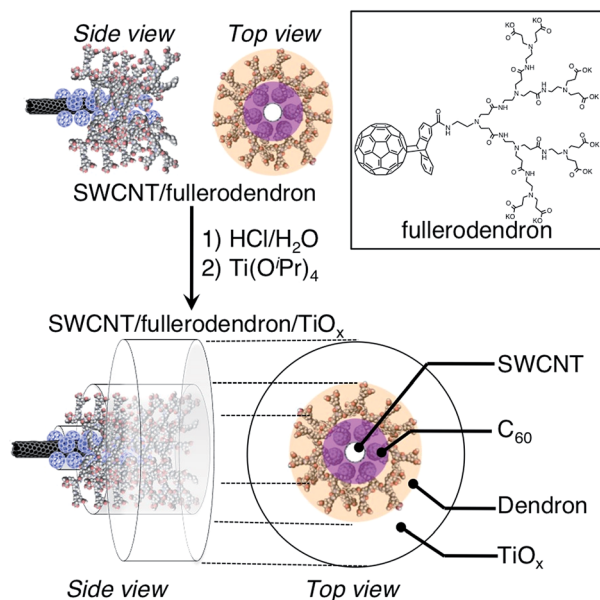


Fig. 1 Schematic illustration of the fabrication of SWCNT/fullerodendron/TiO<sub>x</sub> coaxial hybrid nano-wires.

(250  $\mu$ L: the content of SWCNT is 0.025 mg, 2.0  $\mu$ mol as a C atom) was diluted with water (750  $\mu$ L). The pH was adjusted to pH 3 with HCl (1.0 N, 2.8  $\mu$ L). After the stirring for 1 h, an EtOH solution of titanium tetra isopropoxide (3.51 mM, 20  $\mu$ L,  $7.4 \times 10^{-8}$  mol) was added to the solution at 0  $^{\circ}$ C and stirred for 48 h to obtain a dispersion of SWCNT/fullerodendron/TiO<sub>x</sub> coaxial nanohybrids.

The morphology of the SWCNT/fullerodendron/TiO<sub>x</sub> nano-hybrids was examined by scanning electron microscopy (SEM). The SEM images exhibited SWCNT/fullerodendron/TiO<sub>x</sub> nanowires that are similar to SWCNT/fullerodendron/SiO<sub>2</sub> nanowires (Fig. 2).<sup>12</sup> This structural observation is consistent with the results of transmission electron microscopy (TEM; Fig. S1†) and atomic force microscopy (AFM) measurements (Fig. S2†). The TEM analysis indicated that a uniformly thick shell composed of nano-sized TiO<sub>x</sub> covered the SWCNT/fullerodendron nano-wire. The height profiles in the AFM analysis revealed that the thickness of SWCNT/fullerodendron/

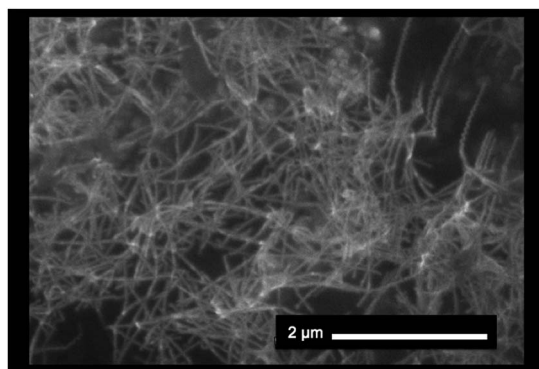


Fig. 2 SEM image of SWCNT/fullerodendron/TiO<sub>x</sub> coaxial nano-hybrids.

TiO<sub>x</sub> coaxial nano-hybrids ( $\sim 15$  nm) is higher than that of the SWCNT/fullerodendron supramolecular nano-composite (2–3 nm).<sup>13</sup> Based on these results, the thickness of the TiO<sub>x</sub> layer was estimated to be 6–7 nm. These observations are consistent with the SWCNT/fullerodendron/TiO<sub>x</sub> coaxial nano-hybrid structure, the SWCNT-core surrounded by the fullerodendrons, coated by the outer TiO<sub>x</sub> shell.

A Raman spectrum of the SWCNT/fullerodendron/TiO<sub>x</sub> coaxial nano-hybrids showed typical scattering of the disorder-induced mode (D) and the tangential displacement mode (TDM; also called the G band), which were observed at 1339 and 1610  $\text{cm}^{-1}$ , respectively (Fig. S3†). The very small intensity of the D-band indicates that the SWCNTs within the composites did not sustain any substantial damage. Broad peaks at 610 and 425  $\text{cm}^{-1}$  were ascribed to TiO<sub>x</sub>. To obtain a better understanding of the fullerodendron/TiO<sub>x</sub> junction, FT-IR spectroscopic measurements of the SWCNT/fullerodendron/TiO<sub>x</sub> nano-hybrid were conducted (Fig. S4†). The IR spectra of the SWCNT/fullerodendron/TiO<sub>x</sub> nano-hybrids exhibit the C=O stretching modes at 1725  $\text{cm}^{-1}$ , which is shifted toward higher frequencies than those of the SWCNT/fullerodendron supramolecular nano-composites (1680  $\text{cm}^{-1}$ ). This result indicates the formation of Ti-OCOR bonds<sup>16</sup> at the termini of the fullerodendrons. The sharp absorption band observed at 635  $\text{cm}^{-1}$  was ascribed to the Ti-O-Ti moieties, while the strong absorption band at 1055  $\text{cm}^{-1}$  was attributed to the Ti-O-C stretching mode. Based on these observations, we concluded that the TiO<sub>x</sub> layer is attached onto the surface of the SWCNT/fullerodendron supramolecular nano-composites without significant damage to the SWCNTs.

The TiO<sub>x</sub> layer of the SWCNT/fullerodendron/TiO<sub>x</sub> nano-hybrids shows high optical transparency in the visible and near infrared (NIR) region. Fig. 3a and S5† show the absorption spectra of the SWCNT/fullerodendron supramolecular nano-composites and the SWCNT/fullerodendron/TiO<sub>x</sub> coaxial nano-hybrids. The absorption of the SWCNT/fullerodendron/TiO<sub>x</sub> coaxial nano-hybrids is smaller than that of the SWCNT/fullerodendron composites, as the concentration of the SWCNT/fullerodendron/TiO<sub>x</sub> coaxial nano-hybrids was lowered during the sol-gel condensation process. However, the absorption and/or scattering due to the TiO<sub>x</sub> layer on the shell should be negligible on account of the nano-sized thickness of the TiO<sub>x</sub> layer. The coaxial nanowire structure with isolated SWCNTs was confirmed by three-dimensional photoluminescence (PL) intensity mapping in D<sub>2</sub>O (Fig. 3b), which allowed assigning four intense peaks with reasonable certainty to the (9,4), (8,6), (7,6), and (8,4) SWCNTs. It should be noted that the coaxial structure is maintained, *i.e.*, the formation of bundles and/or aggregation of the SWCNTs after the formation of the SWCNT/fullerodendron/TiO<sub>x</sub> coaxial nano-hybrids was not observed.

To probe the beneficial aspects of the incorporation of the transparent electron-extraction layer into an SWCNT/fullerodendron coaxial photosensitizer, we explored the photocatalytic evolution of H<sub>2</sub> from water using a system based on the SWCNT/fullerodendron/TiO<sub>x</sub> supramolecular nano-composites coupled with colloidal poly(vinylpyrrolidone)-platinum (PVP-Pt).<sup>17</sup> Typically, 150 mL of an aqueous solution,



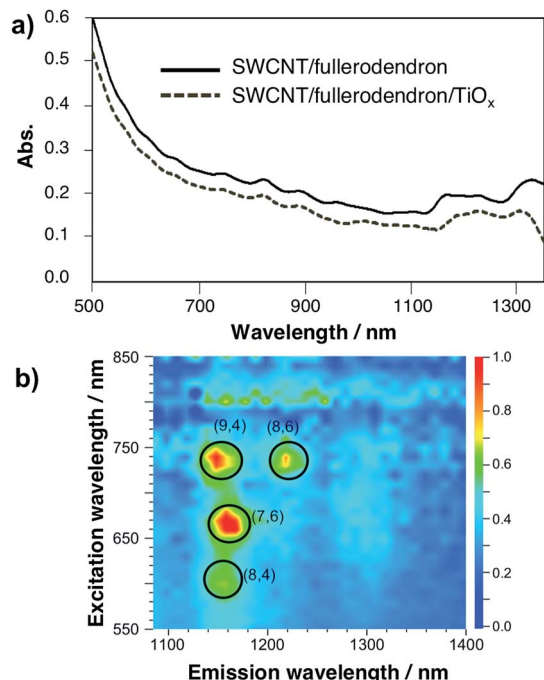


Fig. 3 (a) Vis-NIR spectra of SWCNT/fullerodendron supramolecular nano-composites and SWCNT/fullerodendron/TiO<sub>x</sub> coaxial nano-hybrids. (b) Three-dimensional fluorescence spectra of SWCNT/fullerodendron/TiO<sub>x</sub> coaxial nano-hybrids.

consisting of SWCNT/fullerodendron/TiO<sub>x</sub> nano-composites (1 mL), Tris-HCl buffer (3.5 mL in H<sub>2</sub>O, pH = 7.5, 5 mM), methyl viologen dichloride (MV; 92.4 mg, 359 μmol), 1-benzyl-1,4-dihydronicotinamide (BNAH; 38.6 mg, 180 μmol), and a colloidal solution of PVP-Pt (15 mL in H<sub>2</sub>O; 512 μmol of Pt), was vigorously stirred at 25 °C while being exposed to light ( $\lambda > 422$  nm) from a 300 W Xe arc lamp. After the designated period, the gas phase above the solution was analyzed by gas chromatography. Fig. 4 shows the plots of the total amount of H<sub>2</sub> produced as a function of time using either SWCNT/fullerodendron/TiO<sub>x</sub> coaxial nano-hybrids (◆) or SWCNT/fullerodendron composites (▲). The generation of H<sub>2</sub> (4.0 μmol h<sup>-1</sup>) proceeded steadily and an induction period or decreasing activity was not observed during 6 h of irradiation.

Although the SWCNT/fullerodendron supramolecular nano-composites also worked as a photosensitizer for the evolution of H<sub>2</sub>, the reaction rate of the H<sub>2</sub> generation (1.9 μmol h<sup>-1</sup>; Fig. 3) is lower than that of SWCNT/fullerodendron/TiO<sub>x</sub> nano-hybrids (4.0 μmol h<sup>-1</sup>). Given that the absorbance of the SWCNT/fullerodendron/TiO<sub>x</sub> nano-hybrids is lower than that of the SWCNT/fullerodendron supramolecular nano-composites, the photocatalytic activity of the SWCNT/fullerodendron/TiO<sub>x</sub> nano-hybrids must be higher than that of the SWCNT/fullerodendron supramolecular nano-composites. In order to compare the efficiency of the photocatalytic evolution of H<sub>2</sub> between the SWCNT/fullerodendron supramolecular nano-composite and the SWCNT/fullerodendron/TiO<sub>x</sub> nano-hybrid photocatalysts, we evaluated their quantum yields by using monochromatic light ( $\lambda = 450 \pm 2$  nm), which revealed apparent

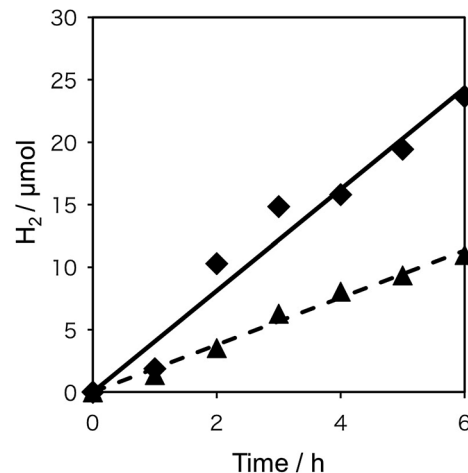


Fig. 4 Time dependence of the evolution of H<sub>2</sub> from water using SWCNT/fullerodendron (▲) or SWCNT/fullerodendron/TiO<sub>x</sub> (◆). Conditions: [MV<sup>2+</sup>]<sub>0</sub> = 359 μmol, [BNAH]<sub>0</sub> = 180 μmol, [Tris-HCl buffer]<sub>0</sub> = 5 mM (pH = 7.5), [PVP-Pt]<sub>0</sub> = 512 μmol, V = 150 mL; vigorous stirring at 25 °C under exposure to light ( $\lambda > 422$  nm) from a 300 W Xe arc lamp.

quantum yields (AQYs) for the evolution of H<sub>2</sub> (2 × number of molecules of H<sub>2</sub> generated/number of photons absorbed) of 0.47 (SWCNT/fullerodendron/TiO<sub>x</sub>) and 0.12 (SWCNT/fullerodendron). By changing the reaction time of sol-gel condensation, it seems that we can control the thickness of TiO<sub>x</sub> layer on the SWCNT/fullerodendron supramolecular nano-composites as judged by the SEM images (Fig. S6†). The photocatalytic activity of SWCNT/fullerodendron/TiO<sub>x</sub> nano-hybrids is affected by the reaction time of sol-gel condensation. The reaction rate of the H<sub>2</sub> generation were 0.1 μmol h<sup>-1</sup> (for 1 day condensation), 4.0 μmol h<sup>-1</sup> (for 2 day condensation), and 0.1 μmol h<sup>-1</sup> (for 3 day condensation), respectively. The SWCNT/fullerodendron/TiO<sub>x</sub> nano-hybrids maintained its photocatalytic activity for at least 12 h. However, the H<sub>2</sub> production rate gradually decreases along with irradiation. The result can be attributed to the decrease of BNAH (sacrificial electron donor) concentration. It is notable that 81% of H<sub>2</sub>-evolving activity was remained for the second use of a spray-coated film of SWCNT/fullerodendron/TiO<sub>x</sub> on a FTO plate after the 6 hour H<sub>2</sub> evolution reaction upon illumination followed by the rinsing and drying.

An energy-level diagram of the conduction (C<sub>1</sub> and C<sub>2</sub>) and valence bands (V<sub>1</sub> and V<sub>2</sub>) of (7,6) SWCNT,<sup>18</sup> which is one of the most commonly encountered types of CNTs in HiPco, together with the LUMO levels of C<sub>60</sub>,<sup>19</sup> MV<sup>2+</sup>,<sup>20</sup> BNAH,<sup>21</sup> and the energy level of Pt and TiO<sub>x</sub> is shown in Fig. 5. A distinctive advantage of the coaxial architecture is that the carrier separation occurs in the shorter radial direction as opposed to the longer axial direction. Moreover, the energy-level diagram indicates that the electron-extraction layer of TiO<sub>x</sub> not only decelerates the electron back-transfer, but also accelerates the electron forward-transfer from the conduction band of TiO<sub>x</sub> to the LUMO of MV<sup>2+</sup>, thus leading to an efficient electron-transfer pathway.





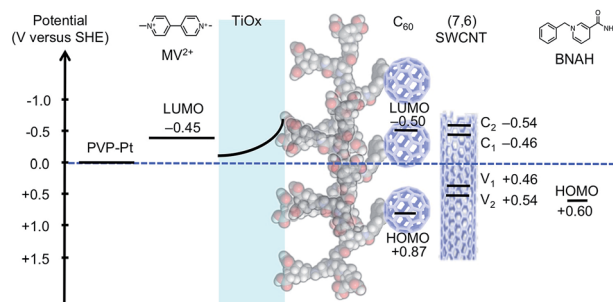


Fig. 5 Energy-level diagram of the SWCNT/fullerodendron/TiO<sub>x</sub> coaxial photocatalyst system.

A bespoke SWCNT photocatalyst with an electron-extracting TiO<sub>x</sub> shell was fabricated. On account of the presence of the TiO<sub>x</sub> shell, the SWCNT/fullerodendron/TiO<sub>x</sub> coaxial nanowire exhibits a high activity in the catalytic evolution of H<sub>2</sub> from water under irradiation with visible light, because the electron-extracting TiO<sub>x</sub> layer accelerates the electron forward-transfer under concomitant deceleration of the undesirable electron back-transfer. Even though various kinds of organic and inorganic coaxial nanowires have been developed so far, coaxial nanowire photocatalysts consisting of (p-type semiconductor)/(n-type semiconductor)/(electron-extraction layer) are still in the early stages of development, mostly due to their relatively complicated fabrication procedures. Further studies on the applications of such SWCNT photocatalysts with coaxial nanowire structures are currently in progress, and will be reported in due course.

## Acknowledgements

This work was partially supported by JSPS KAKENHI grants 15H03519 (Y. T.) and 16K05895 (T. T.).

## References

- For reviews, see: (a) J. Meyer, S. Hamwi, M. Kröger, W. Kowalsky, T. Riedl and A. Kahn, *Adv. Mater.*, 2012, **24**, 5408; (b) K. Zilberberg, J. Meyer and T. Riedl, *J. Mater. Chem. C*, 2013, **1**, 4796; (c) E. L. Ratcliff, B. Zacher and N. R. Armsrong, *J. Phys. Chem. Lett.*, 2011, **2**, 1337.
- (a) S. Tokito, K. Noda and Y. Taga, *J. Phys. D: Appl. Phys.*, 1996, **29**, 2750; (b) H. Kanno, R. J. Holmes, Y. Sun, S. Kena-Cohen and S. R. Forrest, *Adv. Mater.*, 2006, **18**, 339; (c) K. J. Reynold, J. A. Barker, N. C. Greenham, R. H. Friend and G. L. Frey, *J. Appl. Phys.*, 2002, **92**, 7556; (d) C.-W. Chu, C.-W. Chen, S.-H. Li, E. H. E. Wu and Y. Yang, *Appl. Phys. Lett.*, 2005, **86**, 253503; (e) H. You, Y. Dai, Z. Zhang and D. Ma, *J. Appl. Phys.*, 2007, **101**, 026105; J. Meyer, S. Hamwi, M. Kröger, W. Kowalsky, T. Riedl and A. Kahn, *Adv. Mater.*, 2012, **24**, 5408. (f) H. J. Bolink, E. Coronado, D. Repetto, M. Sessolo, E. M. Barea, J. Bisquert, G. Garcia-Belmonte, J. Prochazka and L. Kavan, *Adv. Funct. Mater.*, 2008, **18**, 145.
- For reviews, see: (a) F. Wang, Z. Tan and Y. Li, *Energy Environ. Sci.*, 2015, **8**, 1059; (b) S. Chen, J. R. Manders, S.-W. Tsang and F. So, *J. Mater. Chem.*, 2012, **22**, 24202.
- S. Cho, J. H. Seo, K. Lee and A. J. Heeger, *Adv. Funct. Mater.*, 2009, **19**, 1459.
- C. Waldauf, M. Morana, P. Denk, P. Schilinsky, K. Coakley, S. A. Choulis and C. J. Brabec, *Appl. Phys. Lett.*, 2006, **89**, 233517.
- T. Kuwabara, T. Nakayama, K. Uozumi, T. Yamaguchi and K. Takahashi, *Sol. Energy Mater. Sol. Cells*, 2008, **92**, 1476.
- (a) B. M. Kayes, H. A. Atwater and N. S. Lewis, *J. Appl. Phys.*, 2005, **97**, 114302; (b) Y. Zhang, L. W. Wang and A. Mascarenhas, *Nano Lett.*, 2007, **7**, 1264.
- (a) B. Tian, X. Zheng, T. J. Kempa, Y. Fang, N. Yu, G. Yu, J. Huang and C. M. Lieber, *Nature*, 2007, **449**, 885; (b) Y. Dong, B. Tian, T. J. Kempa and C. M. Lieber, *Nano Lett.*, 2009, **9**, 2183; (c) K.-Q. Peng and S.-T. Lee, *Adv. Mater.*, 2011, **23**, 198; (d) T. J. Kempa, R. W. Day, S.-K. Kim, H.-G. Park and C. M. Lieber, *Energy Environ. Sci.*, 2013, **6**, 719; (e) N. Zhang, M.-Q. Yang, Y. Sun and Y.-J. Zu, *Chem. Rev.*, 2015, **115**, 10307; (f) S. Liu, C. Han, Z.-R. Tang and Y.-J. Xu, *Mater. Horiz.*, 2016, **3**, 270; (g) L. Yuan, C. Han, M.-Q. Yang and Y.-J. Xu, *Int. Rev. Phys. Chem.*, 2016, **35**, 1; (h) C. Han, Z. N. Xhang and Y.-J. Zu, *Nano Today*, 2016, **11**, 351.
- Y. Takaguchi, M. Tamura, Y. Sako, Y. Yanagimoto, S. Tsuboi, T. Uchida, K. Shimamura, S. Kimura, T. Wakahara, Y. Maeda and T. Akasaka, *Chem. Lett.*, 2005, **34**, 1608.
- A. S. D. Sandanayaka, Y. Takaguchi, T. Uchida, Y. Sako, Y. Morimoto, Y. Araki and O. Ito, *Chem. Lett.*, 2006, **35**, 1188.
- A. S. D. Sandanayaka, Y. Takaguchi, Y. Sako, M. Tamura and O. Ito, *Adv. Sci. Lett.*, 2010, **3**, 353.
- T. Tajima, W. Sakata, T. Wada, A. Tsutsui, S. Nishimoto, M. Miyake and Y. Takaguchi, *Adv. Mater.*, 2011, **23**, 5750.
- Y. Sasada, T. Tajima, T. Wada, T. Uchida, M. Nishi, T. Ohkubo and Y. Takaguchi, *New J. Chem.*, 2013, **37**, 4214.
- N. Murakami, Y. Tango, H. Miyake, T. Tajima, Y. Nishina, W. Kurashige, Y. Negishi and Y. Takaguchi, *Sci. Rep.*, 2017, **7**, 43445.
- R. M. Pasquarelli, D. S. Ginley and R. O'Hayre, *Chem. Soc. Rev.*, 2011, **40**, 5406.
- F. X. Perrin, V. Nguyen and J. L. Vernet, *J. Sol-Gel Sci. Technol.*, 2003, **28**, 205.
- H. Hirai, Y. Nakao and N. Toshima, *J. Macromol. Sci., Chem.*, 1979, **13**, 1979.
- Y. Tanaka, Y. Hirana, Y. Niidome, K. Kato, S. Saito and N. Nakashima, *Angew. Chem., Int. Ed.*, 2009, **48**, 7655.
- Y. Takaguchi, Y. Sako, Y. Yanagimoto, S. Tsuboi, J. Motoyoshiya, H. Aoyama, T. Wakahara and T. Akasaka, *Tetrahedron Lett.*, 2003, **44**, 5777.
- M. Ito and T. Kuwana, *Electroanal. Chem.*, 1971, **32**, 415.
- X. Q. Zhu, M. T. Zhang, A. Yu, C. H. Wang and J. P. Cheng, *J. Am. Chem. Soc.*, 2008, **130**, 2501.

